



Research papers

Dynamic volume in karst aquifers: Parameters affecting the accuracy of estimates from recession analysis

Mahmoud Abirifard^a, Steffen Birk^{b,*}, Ezzat Raeisi^a, Martin Sauter^c

^a Department of Earth Sciences, Shiraz University, Iran

^b Institute of Earth Sciences, NAWI Graz Geocenter, University of Graz, Heinrichstr. 26, 8010 Graz, Austria

^c Geoscientific Centre, University of Göttingen, Goldschmidtstr. 3, D-37077 Göttingen, Germany



ARTICLE INFO

This manuscript was handled by Jiri Simunek, Editor-in-Chief, with the assistance of Habib Basha, Associate Editor

Keywords:

Dynamic volume
Recession coefficient
Extrapolation
Karst aquifer
Numerical modelling

ABSTRACT

Reliable estimates of the dynamic volume of karst aquifers, i.e. the drainable volume of groundwater, are important in the context of sustainable management and environmental protection of the karst water resources. Extrapolation of the observed recession of spring hydrographs is commonly used as a basis for the estimation of the dynamic volume. However, our understanding concerning the reliability of this approach is still limited. Therefore, the adequacy of this approach is investigated using flow models of hypothetical karst aquifers to assess the deviation of the extrapolated from the real recession curve and identify parameters controlling the extrapolated recession coefficient. The results show that parameters such as the geometry of the catchment area and point recharge have little effect on the accuracy of the estimated dynamic volume. Low extension of the highly conductive zone and increase in specific yield or catchment area with depth of the aquifer result in the underestimation of the dynamic volume. Groundwater abstraction and decrease of specific yield or catchment area with increasing saturated thickness can lead to an overestimation of the dynamic volume. These findings clarify the potential underestimation or overestimation in dynamic volume estimates on the basis of the observed recession characteristics.

1. Introduction

The dynamic volume of a karst aquifer is defined as the volume of groundwater drainable by gravity at the spring (Padilla et al., 1994). Quantitative information about the dynamic volume of a karst aquifer is required for the development and sustainable management of groundwater resources. El-Hakim and Bakalowicz (2007) documented the importance of this information in a region with a complex karst system, where groundwater abstraction is uncontrolled. Similarly, Hartmann et al. (2012) addressed the drastic water shortage of one of the largest fresh water springs in the West Bank, attributed to an overexploitation of the aquifer, i.e. an inappropriate management of the resource. Knowledge of the dynamic volume also allows the assessment of residence times, relevant for the determination of aquifer vulnerability with respect to contamination (Einsiedl, 2005).

The scientific literature provides a number of methods for estimating the dynamic volume, such as:

1. Analysis of residence times by lumped parameter models based on time series of environmental tracers (e.g. Maloszewski et al., 2002; Einsiedl, 2005)
2. Geometric assessment of the water volume based on the saturated rock porosity above the spring outlet level (Atkinson, 1977; Pérez and Sanz, 2011)
3. Analysis of the karst groundwater flow by numerical methods (e.g. Sauter, 1992)
4. Analysis of the spring discharge recession based on functional relationships such as those proposed by Maillet (1905), Mangin (1975), Padilla et al. (1994), El-Hakim and Bakalowicz (2007), and Mohammadi and Shoja (2014). Some authors also employed hydrological models for this purpose (Fleury et al., 2007; Jukić and Denić-Jukić, 2009; Željkočić and Kadić, 2015; Fu et al., 2016).

The first method requires long-term time series of the relative abundance of stable water isotopes that is often not readily available and inapplicable for many practical purposes. Furthermore, the isotope signal at the spring is dampened considerably for large catchments with

* Corresponding author.

E-mail address: steffen.birk@uni-graz.at (S. Birk).

<https://doi.org/10.1016/j.jhydrol.2022.128286>

Received 10 March 2022; Received in revised form 6 July 2022; Accepted 27 July 2022

Available online 6 August 2022

0022-1694/© 2022 The Author(s). Published by Elsevier B.V. This is an open access article under the CC BY license (<http://creativecommons.org/licenses/by/4.0/>).

large storage volumes. A sufficiently accurate estimate of the effective porosity in karst environments is the most important factor in the application of the second method. Obtaining appropriate estimates of effective porosity in karst aquifers, unfortunately, is highly challenging and typically associated with high uncertainty. Finding the thickness of the phreatic zone between groundwater level and geodetic spring level is another quantity required and regarding the high heterogeneity of karst aquifers it requires groundwater levels, frequently unavailable in karst catchments with thick unsaturated zones. Likewise, the application of numerical flow models requires a wealth of detailed hydrogeological and hydrological data, generally not readily available. For cases where the above mentioned data (environmental tracers, hydraulic heads, etc.) are unavailable, this leaves the fourth method, extrapolating the observed recession and integrating the discharge, as the most attractive approach. [Bakalowicz \(2005\)](#) thus states that there is no other readily applicable method available for evaluating the dynamic volume. Yet, the reliability of the estimates obtained with this method obviously depends on the validity of the extrapolated recession curve. The purpose of this paper, therefore, is to explore for which conditions the extrapolation of the exponential recession function ([Maillet 1905](#)) yields acceptable estimates of the dynamic volume. Further, we want to identify those factors causing either an underestimate or overestimate of the dynamic volume of the aquifer.

In general, various factors and parameters can be assumed to affect the recession coefficient at different times of the discharge recession curve, e.g. at early times the type and distribution of recharge (localized or distributed, intensity and duration, etc.) and the epikarst hydraulics, at intermediate times the hydraulic properties and the spatial extent of the conduit network, and at late times the heterogeneity and hydraulic properties of the aquifer matrix as well as the catchment geometry. The estimation of the dynamic volume mainly depends on the recession at intermediate and late time following the rainy season or recharge event. Therefore, the focus of this research is placed on the identification of factors and parameters affecting the recession coefficient during intermediate and late times of the discharge recession. For this purpose, simplified but realistic, close to nature prototype karst aquifers are designed and implemented in the Conduit Flow Process (CFP) mode of the modular finite-difference ground-water flow model, MODFLOW-2005 ([Shoemaker et al., 2008](#)). The CFP model option simulates flow in discrete conduits and turbulent groundwater flow conditions, as well as the interaction between the conduit network and the permeable aquifer matrix. By changing boundary conditions and aquifer parameters, a sensitivity study is carried out and the effect of a change in selected parameters and factors on the shape of the recession curve and consequently on the dynamic volume is assessed. Thus, we follow the generally accepted approach of applying simplified karst models to improve the understanding and the analysis of the spring discharge recession as already demonstrated by, e.g., [Eisenlohr et al. \(1997\)](#) and [Kovács et al. \(2005\)](#).

2. Material and methods

2.1. Dynamic volume

As discussed above, the analysis of the spring discharge recession based on functional relationships is a widely used and practical method for calculating the dynamic volume of the karst aquifer. [Dewandel et al. \(2003\)](#) and [Fiorillo \(2014\)](#) published comprehensive review papers on this topic. The Maillet formula, an exponential equation widely used for recession curve analysis, is an approximate analytical solution for the diffusion equation ([Dewandel et al., 2003](#)). Here, it is used for the estimation of the dynamic volume. The actual dynamic volume of the simplified prototype model karst aquifer is calculated based on mass storage in the aquifer using the discretized output of the MODFLOW-CFP model. More details about how to calculate the estimated and actual dynamic volume are described below.

2.1.1. Estimates of the dynamic volume

The Maillet formula describes the recession using an exponential function of time:

$$Q_R = Q_{R0} e^{-\alpha t}$$

Q_R in m^3/s is the discharge from the phreatic zone, Q_{R0} in m^3/s is the initial discharge at time zero; α in day^{-1} is the recession coefficient, and t is time in days. This allows calculating the dynamic volume, V_{dyn} , in m^3 by integration, which relates to the total volume of drainable water in storage in the saturated zone above the geodetic level of the spring outlet ([Ford and Williams, 2007](#)):

$$V_{dyn} = \int_0^{\infty} Q_{R0} e^{-\alpha t} dt = C \frac{Q_{R0}}{\alpha}$$

C is a constant equal to 86,400, for Q_{R0} being expressed in m^3/s and α in day^{-1} .

The volume of water dynamically stored in the aquifer at the end of the observed recession period (remaining dynamic volume) is more important for aquifer management during extended drought than the total dynamic volume. [Fig. 1](#) shows estimates of the total dynamic volume and the remaining dynamic volume obtained from the Maillet formula. As shown in [Fig. 1](#), the remaining dynamic volume displays some uncertainty because the late recession is not observed due to recharge events. Thus, it is estimated by extrapolation using the recession coefficient from the observed recession period. Therefore, the focus of this research is on calculating estimates of the remaining dynamic volume. To do so, the Maillet formula is fitted to the observed base flow recession of the spring discharge (red solid lines in [Fig. 1](#)). Together with the recession coefficient of this formula and the spring discharge at the initial time of the extrapolation period, the estimate of the remaining dynamic volume was determined.

2.1.2. Actual dynamic volume

The actual dynamic volume remaining at the beginning of the extrapolation period of the hypothetical prototype karst aquifer is calculated based on the storage in this aquifer using the discretized output of the employed groundwater flow model MODFLOW-CFP (see 2.2). This is achieved by adding up the drainable water volume stored in each of the active cells at the start of the extrapolation period. For each cell, this volume is obtained by multiplying the specific yield, the area of the cell, and the saturated thickness, obtained from the simulated hydraulic head.

2.2. Numerical aquifer model

The discharge recession depends on the interaction between the highly conductive, low storage conduit network system and the less conductive, high storage matrix system. The groundwater flow model MODFLOW-CFP ([Shoemaker et al., 2008](#)), representing the complex hydraulic interaction between conduits and matrix, has been employed to better understand the influence of the aquifer properties on the discharge recession. MODFLOW-CFP is a finite-difference groundwater flow model developed especially for karst aquifers displaying nonlinear or turbulent flow. This code contains three modules, each with unique abilities for simulating different aquifer conditions. Mode 1 is applied to simulate the hydraulic response of a discrete pipe network imbedded in a low permeability carbonate rock matrix. Mode 2 considers a preferential flow layer with the ability of switching between laminar and turbulent conditions. Mode 3 mixes the preferential flow layer with a pipe network. CFP mode 1 has especially been designed to simulate groundwater flow in a conduit network with defined dimensions. It requires information about conduit geometry and hydraulic properties. CFP mode 2 is effectively applicable to simulate less mature karst aquifers without a well-developed network of conduits and pipes or without detailed information about the properties of the conduit system.

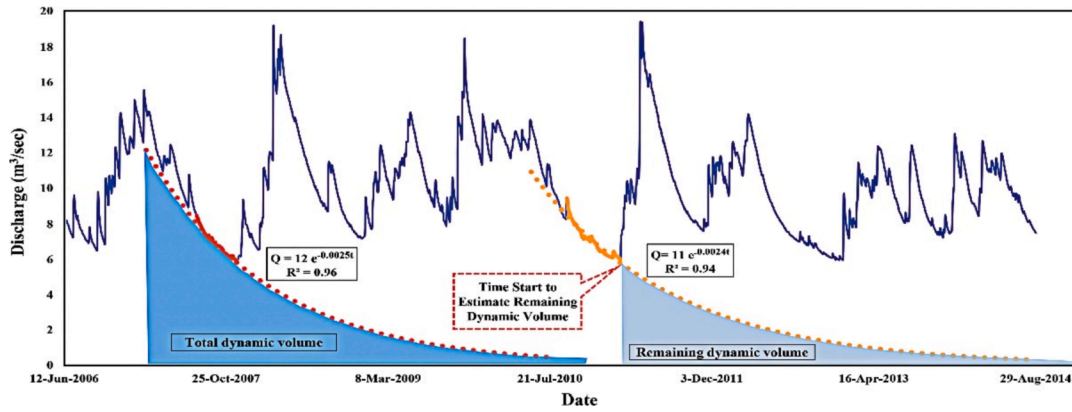


Fig. 1. Total and remaining dynamic volume of the Mammoth Spring (using World Karst Spring hydrograph database (Olarinoye et al., 2020)).

Its dependence on just a few parameters such as the critical Reynolds numbers, and void diameters, is one of the most important advantages of this mode. Thus, CFP mode 2 is employed here.

CFP mode 2 considers non-Darcian flow conditions in lateral flow, but not in vertical direction. Using MODFLOW-CFP mode 2, the effect of non-laminar and turbulent flow is considered by reducing the hydraulic conductivity with increasing flow velocity once the critical Reynolds number, indicating the transition from Darcian to non-Darcian flow, is exceeded (Kuniansky et al., 2008).

2.2.1. Parameter study

Various parameters and factors affect the shape of the recession curve such as hydraulic conductivity, specific yield and aquifer geometry (Kovács et al., 2005; Dewandel et al., 2003; Bonacci, 1993), mode of recharge (Smart and Hobbs, 1986) and conduit network density (Eisenlohr et al., 1997). Changes in recession coefficient on the falling limb of the spring hydrograph can be related to flow regimes with different magnitudes of hydraulic conductivity (Forkasiewicz and Paloc, 1967; Baedke and Krothe, 2001), changes in the catchment area or effective porosity with depth of aquifer (Fiorillo, 2011, 2014) and the duration of the recharge pulse (Birk and Hergarten, 2010). Groundwater abstraction in the catchment area and delayed or ongoing recharge from the vadose zone (Wu et al., 2019; Eisenlohr et al., 1997; Perrin, 2003; Lastennet and Mudry, 1997) result in an increase and decrease of the recession coefficients, respectively. Below, we developed different scenarios to simulate the above cases and examine the influence of the characteristics of each case on the recession coefficient and the dynamic volume.

2.2.2. Basic model setup and modifications

The hypothetical spring catchment includes a fissured limestone matrix, drained by a highly conductive zone, represented by a single conduit. As Fig. 2 shows, this model is discretized into 30 rows and 50 columns. The width of the columns and rows is 100 m except where cells are close to the highly conductive zone. The length of the highly conductive zone is 4000 m; its thickness and width are 2 m and 1 m, respectively. The catchment is delineated by a no-flow (Neumann type) boundary, except for the spring location, represented by a fixed head boundary condition at 2 m (Dirichlet type boundary). The basic geometry used here is an upscaled and modified version of a MODFLOW-CFP setup previously used for other parameter studies (Birk et al., 2006; Reimann et al., 2011). Since unconfined groundwater flow was modeled, the horizontal transmissivity is a function of the saturated thickness of the cells. Throughout the simulation, MODFLOW-CFP computes the saturated thickness for the individual cells. If the saturated thickness becomes zero, MODFLOW converts the cell into dry cells (no flow).

Recharge (500 mm/y) infiltrates during a 5-month precipitation period (corresponding to precipitation patterns recorded in South-Central Iran (Naderi and Raeisi, 2015)). The discharge of the large karst springs in Iran starts to increase with the beginning of the wet season and starts to decrease at the end of this period (Mohammadi and Shoja, 2014; Kavousi and Raeisi, 2015). Based on this behavior, recharge increases in the model linearly and becomes zero at the end of the precipitation season (Fig. 3).

While recharge is spatially uniformly distributed in the basic scenario, some modified scenarios consider the effect of localized recharge directly into sinkholes. For these scenarios, 5 % of total recharge is

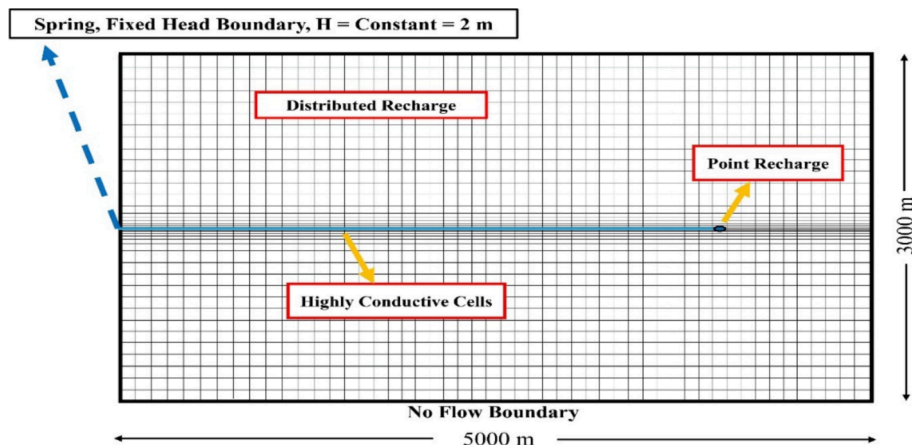


Fig. 2. Plan view of the model domain showing highly conductive cell (conduit) embedded in a matrix system.

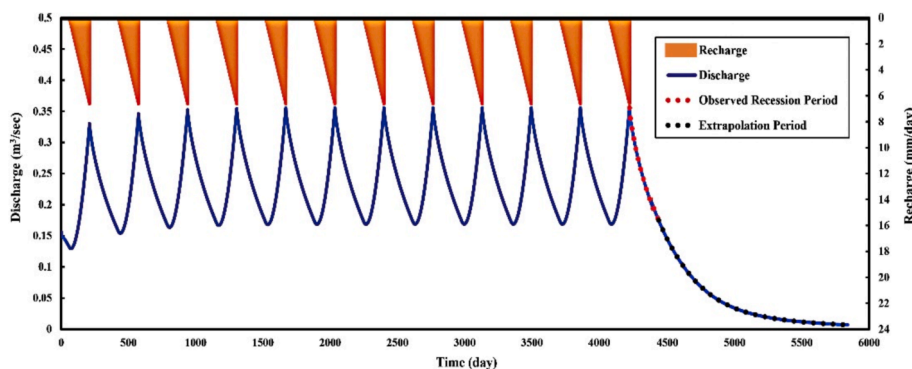


Fig. 3. Time-series of recharge input and modelled spring discharge. During the final long-term recession, the observed recession period and the extrapolation period are depicted.

directly injected into the first cell of the highly conductive zone and the remaining 95 % are distributed across the low-permeability matrix. The hydraulic parameters are uniform both within the low-permeability matrix and within the highly conductive zone. A value of 10^{-4} ms^{-1} is defined as hydraulic conductivity of the matrix; its specific yield is 0.02. The hydraulic conductivity of the highly conductive zone is 147 ms^{-1} , which corresponds to a 0.2 m diameter pipe computed by the Hagen-Poiseuille formula (Reimann et al., 2011). Upper and lower limits of the critical Reynolds number for the threshold between Darcian and non-Darcian flow conditions are 50 and 100, respectively. Table 1 depicts how the basic scenario (S_1) is modified in the model scenarios considered here. The simulation time period is 16 years for all scenarios in Table 1. During this time period, 12 years have recharge periods and in the remaining 4 years recharge is defined as zero to simulate a long-term recession (Fig. 3). At first, all scenarios have been run in steady-state mode with constant recharge depth; then transient recharge was applied starting with the steady-state head distribution as initial condition.

3. Model results

The simulated discharge during the recession period is shown for three example scenarios in Fig. 4a, b and c. Supplement 1 provides the corresponding figures for the full set of scenarios. Fig. 4a shows the discharge in a semi-logarithmic plot for the basic scenario (S_1). This scenario resulted in an almost straight line (except for negligible differences in the beginning of the graph) indicating exponential decrease in discharge during the recession period. The same recession behavior is apparent in the scenarios assuming point recharge (S_3), point recharge at short distance from the spring (S_4), and different length and width ratios of the aquifer (1 and 4; S_{17} and S_{18}) (see Supplement 1). Fig. 4b displays the discharge recession for the scenario with reduced spatial extent of the highly conductive zone (S_5). The concave shape of the discharge recession indicates the discharge decreases slower than exponential decay with time. This is also found for the scenarios with higher critical Reynold Number (S_6), increase and decrease in hydraulic conductivity with depth of aquifer (S_8 , S_9), increase in hydraulic conductivity in length of aquifer (S_{10}), increase in specific yield with depth of aquifer (S_{12}), increase in catchment area with depth of aquifer (S_{14}) and increase in hydraulic conductivity of the highly conductive zone (S_{16}) (see Supplement 1). The scenarios with ongoing recharge (S_2) displays a convex shape implying that discharge decreases faster than exponential decay with time (Fig. 4c). This is obtained from scenarios with exploitation well (S_7), decrease in hydraulic conductivity in downgradient direction of the aquifer (S_{11}), decrease in specific yield with decreasing depth of the aquifer (S_{13}) and decrease in catchment area with decreasing depth of the aquifer (S_{15}) (see Supplement 1).

Based on the recession coefficient of the observation period and the discharge at the initial time of extrapolation period, the estimated

remaining dynamic volume was calculated (Table 2). Table 2 also provides the exponential fit equation R^2 , and actual remaining volume.

Fig. 5a compares the estimated and the actual remaining dynamic volumes. Fig. 5b shows the relative error of the estimated remaining dynamic volumes. Comparing scenarios, it becomes obvious that the actual dynamic volume increases with an increase in specific yield, with increasing distance between the point of recharge and the spring, with increasing catchment area, with ongoing recharge and with a decrease in hydraulic conductivity of the matrix and conduit, with an increase in spatial extent of the highly conductive zone, with an increase in critical Reynolds numbers and with increasing percentage of point recharge. For these conditions, the karst aquifer can sustain flow for a long time period and is therefore much less affected by dry seasons and long-term droughts. For inverse conditions, the dynamic volume of the aquifer decreases and thus the aquifer is more subject to the adverse effects of droughts (Fiorillo et al., 2012). Following Fiorillo et al. (2012) karst springs that have large dynamic volume can be termed drought resistant, whereas those with a small volume are drought vulnerable. Over-estimation or underestimation of the dynamic volume thus may result in misjudgment of the resistance or vulnerability of a karst spring to drought.

4. Discussion

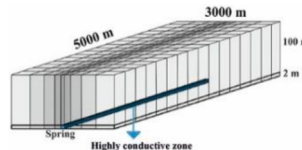
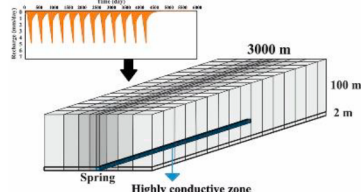
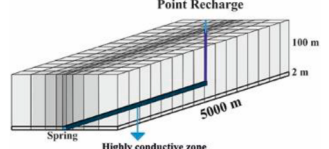
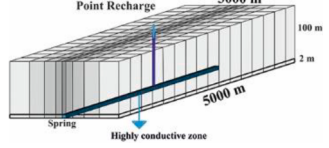
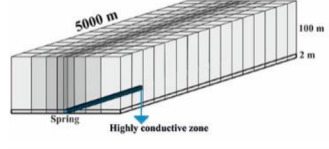
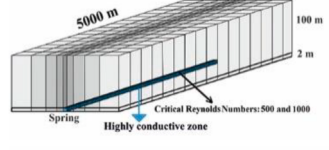
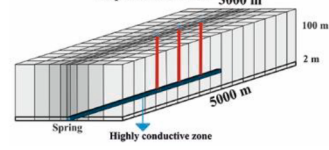
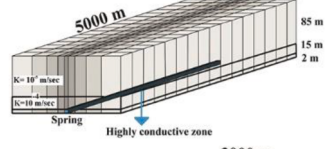
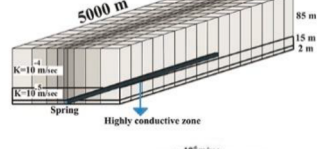
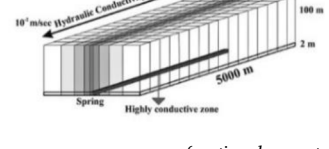
Table 3 provides information on the characteristics of some karst springs in the Zagros Mountains of Iran. As shown in this table, these springs have different recession coefficients and dynamic volumes (estimated based on recession analysis). In order to improve our understanding of the origin of such differences and to assess potential errors in the estimation of the dynamic volumes, this section discusses the results of the scenario investigations and compares them with selected real-world examples.

As mentioned above, different scenarios show three groups of parameters: a) parameters with no (or little) contribution to the error in the estimation of dynamic volume, b) parameters likely to contribute to an underestimation, and c) parameters possibly contributing to an over-estimation of the dynamic volume. The role of the above parameters is discussed below.

4.1. Parameters contributing little to the error in the estimation of the dynamic volume

The basic scenario as well as scenarios considering point recharge (S_3 , S_4) and different geometry of the catchment area (L/W ratio; S_{17} , S_{18}) exhibit only minor deviations between the recession curve extrapolated based on the Maillet equation and the observed recession (Fig. 4a and Supplement 1). As a result, these factors do not notably affect the estimation of the remaining dynamic volume and do not add any error in dynamic volume estimation based on an extrapolation of the observed

Table 1
Factors and parameters varied compared to the basic scenario.

Scenarios	Geometry, parameters and factors changed in the model setup	Schematic of the Scenarios
Basic scenario	Model setup for this scenario described in the context (S ₁)	
Ongoing recharge	Changes in the recharge function such that 30 % of recharge occurs during the recession period and decreases exponentially (S ₂)	
Point recharge	5 % of total recharge is point recharge into the highly conductive zone (S ₃)	
	5 % of total recharge is point recharge into the highly conductive zone and point recharge locations at low distances from the spring (S ₄)	
Extension high conductive zone	Reducing the length of the highly conductive zone from 4000 m in the basic scenario to 1000 m in this scenario (S ₅)	
Critical Reynolds number	Increasing the critical Reynolds numbers from 50 and 100 in the basic scenario to 500 and 1000 in this scenario (S ₆)	
Exploitation well	Considering three pumping wells with an extraction rate of 10 l/s in model (S ₇)	
Changing hydraulic conductivity with depth of aquifer	Considering two layers above the spring with upper and lower layers hydraulic conductivity of 10 ⁻⁵ ms ⁻¹ and 10 ⁻⁴ ms ⁻¹ , respectively (S ₈)	
	Considering two layers above the spring with upper and lower layers hydraulic conductivity of 10 ⁻⁴ ms ⁻¹ and 10 ⁻⁵ ms ⁻¹ , respectively (S ₉)	
Changing hydraulic conductivity with distance towards the spring	Gradual increase of matrix hydraulic conductivity along the aquifer from 10 ⁻⁶ ms ⁻¹ to 10 ⁻² ms ⁻¹ (S ₁₀)	

(continued on next page)

Table 1 (continued)

Scenarios	Geometry, parameters and factors changed in the model setup	Schematic of the Scenarios
	Gradual decrease of matrix hydraulic conductivity along the aquifer from 10^{-2} ms^{-1} to 10^{-6} ms^{-1} (S_{11})	
Changing specific yield with depth of aquifer	Considering two layers above the spring with the upper and lower layer specific yield of 0.01 and 0.1, respectively (S_{12})	
	Considering two layers above the spring with the upper and lower layer specific yield of 0.1 and 0.01, respectively (S_{13})	
Changing catchment area with depth of aquifer	Increase in catchment area of the aquifer with depth (S_{14})	
	Decrease in catchment area of the aquifer with depth (S_{15})	
Changing hydraulic conductivity high conductive zone	Increase in hydraulic conductivity of the highly conductive zone from 147 ms^{-1} in the basic scenario to 294 ms^{-1} in this scenario (S_{16})	
Catchment area shape	Change in length and width ratio of aquifer (L/W) to 1 (S_{17}) (In this scenario, the model domain is $4000 \text{ m} \times 4000 \text{ m}$ and highly conductive zone length is 3000 m)	
	Change in length and width ratio of aquifer (L/W) to 4 (S_{18}) (In this scenario, the model domain is $8000 \text{ m} \times 2000 \text{ m}$ and highly conductive zone length is 7000 m)	

recession.

In scenario S_3 , 5 % of recharge was allocated as point recharge directly into the highly conductive zone. The recession coefficient of the exponential fit to the base flow of S_3 (0.0033d^{-1}) is slightly higher than that of the basic scenario (0.0032d^{-1}). This is caused by the direct connection of this recharge component to the highly conductive zone, explaining the slightly more rapid drainage of the aquifer. The actual dynamic volume remaining at the beginning of the extrapolation period thus is smaller than that of the basic scenario. Yet, the modeling results reveal that the recession curve extrapolated from the observed recession is very close to the actual spring discharge through the extrapolation period. Therefore, the estimation of the remaining dynamic volume is found to be reliable. For the S_4 scenario, in which the distance between

the point of recharge and the spring decreases, the recession coefficient of the base flow exponential fit is slightly increased compared to the basic scenario from 0.0032d^{-1} to 0.0033d^{-1} . Thus, the dynamic volume in S_4 is larger than that of the basic scenario, but again the estimated remaining dynamic volume is reliable.

Likewise, for scenarios S_{17} and S_{18} , investigating the effect of basin geometry, the discharge recession during the extrapolation period is matched by the Maillet equation that was fitted to the observed recession period. Thus, for each of these scenarios the estimation of the remaining dynamic volume is reliable, although the values of the actual dynamic volumes differ from that of the basic scenario (see Table 1). A larger extent in flow direction of the aquifer (S_{18} where length/width = 4) leads to a lower recession coefficient and thus larger remaining

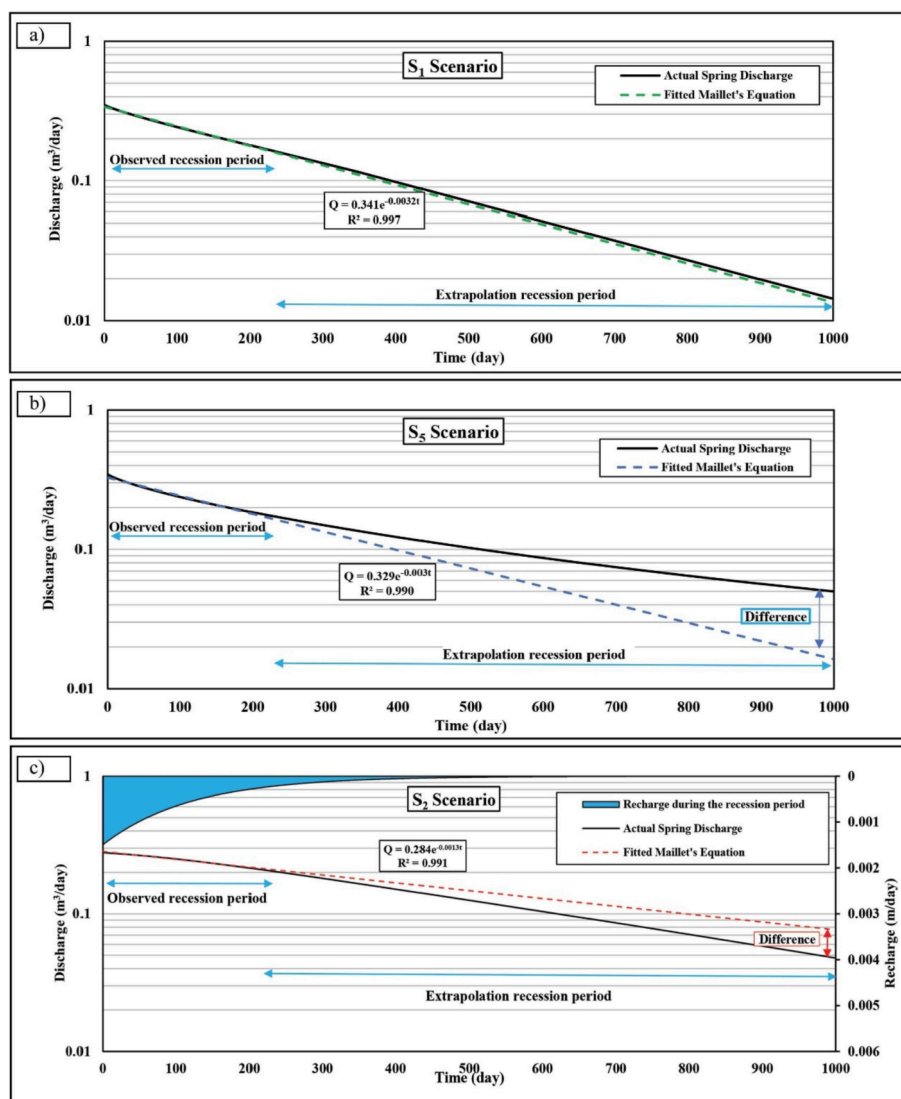


Fig. 4. Examples scenarios a) with constant changing rate of discharge during recession period (S_1); b) with a decreasing changing rate of discharge over time (S_5); c) with an increasing changing rate of discharge over time (S_2). The corresponding figures of the other scenarios are provided by Supplement 1.

Table 2

Estimation of the remaining dynamic volume based on the Maillet equation, fitted to the observed recession period (Fig. 4).

Scenarios	Base flow exponential fit	Recession coefficient (1/day)	R ²	Q at start of extrapolation period (m ³ /s)	Estimated remaining dynamic volume (10 ⁶ m ³)	Actual remaining dynamic volume (10 ⁶ m ³)
S ₁	$0.341e^{-0.0032t}$	0.0032	0.997	0.176	4.8	5.0
S ₂	$0.284e^{-0.0013t}$	0.0013	0.991	0.213	14.2	10.1
S ₃	$0.339e^{-0.0033t}$	0.0033	0.997	0.175	4.6	4.7
S ₄	$0.335e^{-0.0034t}$	0.0034	0.995	0.171	4.3	4.5
S ₅	$0.329e^{-0.0030t}$	0.0030	0.990	0.181	5.2	9.8
S ₆	$0.418e^{-0.0056t}$	0.0056	0.998	0.133	2.1	3.5
S ₇	$0.318e^{-0.0038t}$	0.0038	0.999	0.143	3.3	2.3
S ₈	$0.300e^{-0.0020t}$	0.0020	0.993	0.198	8.6	12.8
S ₉	$0.352e^{-0.0035t}$	0.0035	0.998	0.169	4.2	6.8
S ₁₀	$0.406e^{-0.0075t}$	0.0075	0.936	0.102	1.2	7.8
S ₁₁	$0.287e^{-0.0015t}$	0.0015	0.999	0.209	12.0	9.4
S ₁₂	$0.433e^{-0.0059t}$	0.0059	0.999	0.128	1.9	6.4
S ₁₃	$0.255e^{-0.0008t}$	0.0008	0.990	0.216	23.3	17.3
S ₁₄	$0.432e^{-0.0087t}$	0.0087	0.978	0.082	0.8	2.5
S ₁₅	$0.216e^{-0.0018t}$	0.0018	0.998	0.149	7.2	4.9
S ₁₆	$0.386e^{-0.0046t}$	0.0046	0.999	0.150	2.8	4.2
S ₁₇	$0.343e^{-0.0026t}$	0.0026	0.998	0.200	6.6	6.9
S ₁₈	$0.326e^{-0.0023t}$	0.0023	0.986	0.207	7.8	8.1

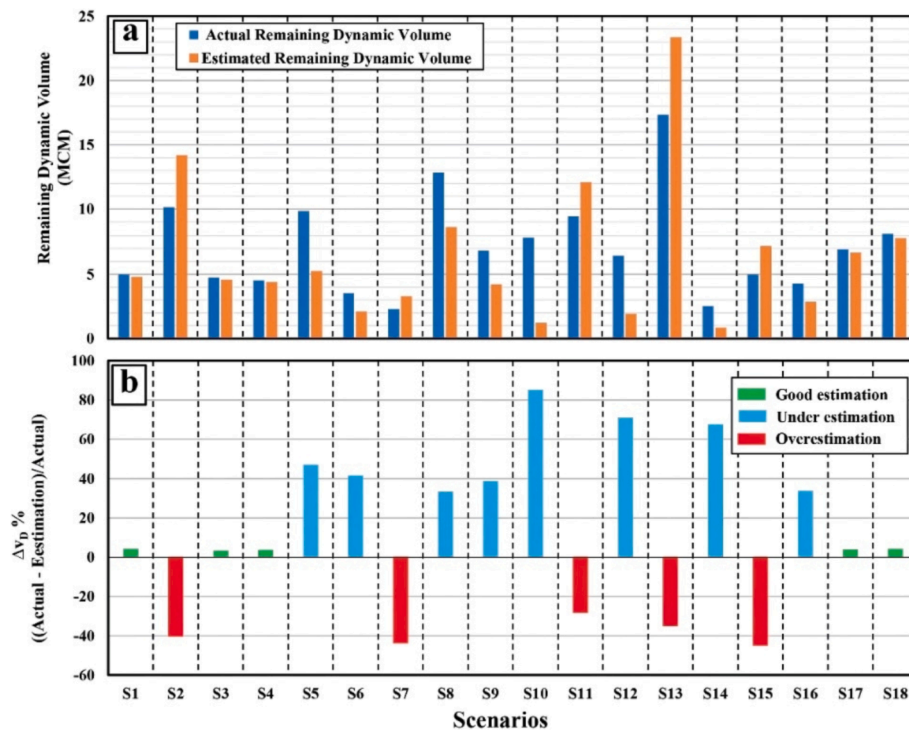


Fig. 5. a) Actual and estimated remaining dynamic volume (based on recession analysis) b) percentual error in the estimation of dynamic volume, for all scenarios.

Table 3

Characteristics of some karst springs in Iran.

Spring	Catchment Area (km ²)	Average Elevation (m)	Average Discharge (m ³ /s)	Annual Precipitation (mm)	α			Dynamic Volume (10 ⁶ m ³)
					α_1	α_2	α_3	
Pireghar ^(a)	102	2794	1.8	606	0.026	0.005	35.9	
Dime ^(a)	140	2590	2.6	1305	0.0032	0.0005	56.9	
Sheshpeer ^(b)	81	2998	3.24	1350	0.0087	0.0018	100*	
Berghan ^(c)	19	2500	0.63	1100	0.006	0.0036	25.6*	
Sasan ^(d)	220	832	1.9	800	0.02	0.009	0.002	97
Gilan ^(e)	110	1413	0.938	625	0.0004	0.0012		84*

(a) Mohammadi and Shoja (2014).

(b) Raeisi et al. (1993).

(c) Raeisi and Karami (1997).

(d) Barmaki et al. (2019).

(e) Karimi et al. (2003).

*Calculated based on data in the paper.

dynamic volume compared to non-expanded settings (S₁₇ with length/width ratio = 1). The density (length/area) of the highly conductive zone in the longer aquifer is larger compared to that in non-expanded one. Nevertheless, the recession coefficient of the non-expanded aquifer is higher and thus the remaining dynamic volume lower. For equal densities of the highly conductive zone, the difference in recession coefficient and remaining dynamic volume is even more increased. In the Gilan Aquifer located in the Zagros Region, West-Iran, employed as an example of a limestone karst aquifer in which despite conduit flow (Karimi et al., 2003), the recession coefficient of the base flow condition is low (0.0012d⁻¹) and the large (ca. 37 km) longitudinal extent provides large volumes of water during the base flow period (72·10⁶ m³). In contrast, the catchment area of the Pireghar Karst Spring in the same region (Zagros Region) and with similar lithological composition (Asmari Formation) but shorter longitudinal extent (21 km), exhibits a higher recession coefficient (0.005 d⁻¹) and lower dynamic volume (21·10⁶ m³) for base flow conditions (Mohammadi and Shoja, 2014). Other characteristics of these two spring catchments are similar. For instance, the catchment areas of the Gilan Aquifer and Pireghar Karst

Spring are 110 km² and 102 km², and average annual precipitation is 625 mm and 606 mm, respectively, suggesting recharge is similar. Based on the model results it is thus suggested that the different geometry in the given examples is a likely reason for the differences in the observed recession coefficients and the values of the actual dynamic volumes, but that the geometry does not affect the reliability of the dynamic volume estimates.

4.2. Parameters causing underestimation of the dynamic volume

During the extrapolation period of some scenarios, the modelled recession coefficient decreases faster than the observed discharge recession coefficient (Fig. 4b). Therefore, the modelled remaining dynamic volume is lower than the actual volume. In many real karst aquifers, the highly conductive zone may not extend throughout the entire aquifer (S₅ scenario) and in most cases these less permeable regions have a considerable extent in areas at remote upgradient distance from the spring outlet. As a result, the behavior of the springs is flashy and during early times, when the drainage of the area close to the spring

initially controls discharge, groundwater drains rapidly from the karst aquifer. However, after draining of this aquifer section, the low-conductive area at greater distance from the spring controls the flow of groundwater. During the extrapolation period, slow groundwater drainage from the remote area thus causes the observed discharge to decrease slower compared to the one modelled using the Maillet equation. In scenario S_5 , the estimated and actual remaining dynamic volumes are $5.2 \cdot 10^6 \text{ m}^3$ and $9.8 \cdot 10^6 \text{ m}^3$, respectively.

A similar effect is obtained when the matrix hydraulic conductivity increases along the aquifer toward the spring. Scenario S_{10} shows that in this case the discharge during the extrapolation period decreases slower than the exponential decay that was fitted to the observed recession period (Supplement 1). Therefore, the estimated remaining dynamic volume is less than the real volume. The matrix hydraulic conductivity in a karst aquifer may also increase or decrease with depth. The S_9 scenario considers two layers where the upper layer has a higher hydraulic conductivity compared to the lower layer, connected to the highly conductive zone. Initially, groundwater is quickly drained from the upper layer, and thus the recession of the spring hydrograph is fast. As this upper layer falls dry, however, only the less conductive lower layer provides flow to the spring. Thus, the discharge from the karst aquifer decreases more slowly than before when the discharge was provided by the upper, more conductive layer. If the drop of the water table to the level of the less conductive layer occurs at the extrapolation stage, the consequence would be an underestimation of the remaining dynamic volume. An example of this type of behavior is apparent in the Gallusquelle karst aquifer in southwest Germany (Sauter, 1992). As shown in Fig. 6, the recession coefficient of the karst spring draining this aquifer is considerably reduced when groundwater level drops below a specific threshold (660 m in B7 and 683 m in B14 observation boreholes). Based on pumping and injection tests data and also well logs, Sauter (1992; 1995) related this change in recession coefficient to a decrease in hydraulic conductivity with depth. Similar observations (such as in S_9 scenario) are made when the hydraulic conductivity of the deep layer is higher compared to that of the shallow one (S_8).

In some karst aquifers, it is possible that the specific yield and catchment area increase with the depth of the aquifer. Scenarios S_{12} and S_{14} consider an increase with depth for the specific yield or the catchment area, respectively. As shown by the modeling results (Supplement 1), for both of these scenarios during the extrapolation period spring discharge decreases slower than the exponential decline fitted to the observed recession period. With the drop of the groundwater level during the recession period, the water volume released per unit head change increases under these conditions. Therefore, the extrapolation based on Maillet's equation leads to an underestimation of the remaining dynamic volume in a real karst aquifer.

In a highly conductive zone turbulent flow conditions can affect the emptying rate of the aquifer and thus the estimation of the remaining dynamic volume of the aquifer. For turbulent flow, a proportion of the energy and head will be lost by energy dissipation in eddies. Thus, the

effective hydraulic conductivity of the conduit for turbulent flow conditions is less than for laminar flow. The parameter commonly used to assess when flow turns from laminar into turbulent is the critical Reynolds number. Conduits with low tortuosity and low internal roughness have larger critical Reynolds numbers, which means that laminar flow prevails in the conduit (Shoemaker et al., 2008). An increase in the critical Reynolds number facilitates the drainage through the highly conductive zone, and thus the drainage of water from areas remote from the spring during the extrapolation period. As a result, spring discharge decreases slower during the extrapolation period of this scenario (S_6) compared to the exponential decline fitted to the observed recession period. Thus, the estimate of the remaining dynamic volume is lower than the actual volume.

Increasing or decreasing the hydraulic conductivity in the highly conductive zone has effects similar to an increase and decrease in the critical Reynolds number. With increased hydraulic conductivity in the highly conductive zone, the emptying rate of the aquifer increases and the dynamic volume decreases and vice versa. In scenario S_{16} with high hydraulic conductivity in the highly conductive zone, the emptying rate of the aquifer is high during observed recession times and decreases during the extrapolation period. Thus, the remaining dynamic volume estimate is lower compared to the actual volume. A good example for showing the effect of a highly conductive zone on the magnitude of the recession coefficient (emptying rate of the aquifer during recession times) and dynamic volume is the Hammerbach spring system. This spring emerges from the Lurbach karst aquifer located in the south of Austria. After a flood event in August 2005, part of the main conduit in this aquifer presumably was plugged with sediments decreasing the effective hydraulic conductivity of the whole system (Mayaud et al., 2016). As a result, the discharge behavior of the Hammerbach spring changed to a more dampened discharge pattern after this event, despite the pattern of precipitation not having been changed. As shown in Fig. 7, the recession coefficient decreased after this event from 0.02 d^{-1} to 0.013 d^{-1} and the dynamic volume of the aquifer increased accordingly.

4.3. Parameters causing overestimation of the dynamic volume

In some scenarios, the curve fitted to the observed recession decreases slower than real discharge recession during the extrapolation period (Fig. 4c). Thus, the dynamic volume is being overestimated. One potential cause of this behavior is that recharge did not entirely cease for some time period of the observed recession. This can be an effect of the hydraulic function of an epikarst. The epikarst zone can be very thick and thus may store significant volumes of water. Water flow from this zone toward the saturated zone via the vadose zone has different velocities (Smart and Friederich, 1987; Kogovsek, 1997; Sauter, 1992). Therefore, part of the epikarst water may flow slowly and reach the phreatic zone delayed during the recession period. To account for such a slow recharge process, the S_2 scenario considers that 30 % of total recharge occurs during the recession period and decreases exponentially

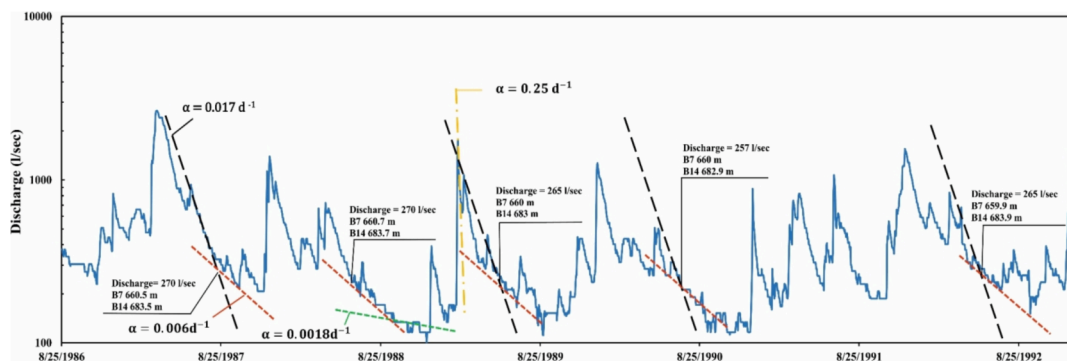


Fig. 6. Change of the recession coefficient at a specific level in the Gallusquelle aquifer due to decreasing matrix hydraulic conductivity (Sauter 1992).

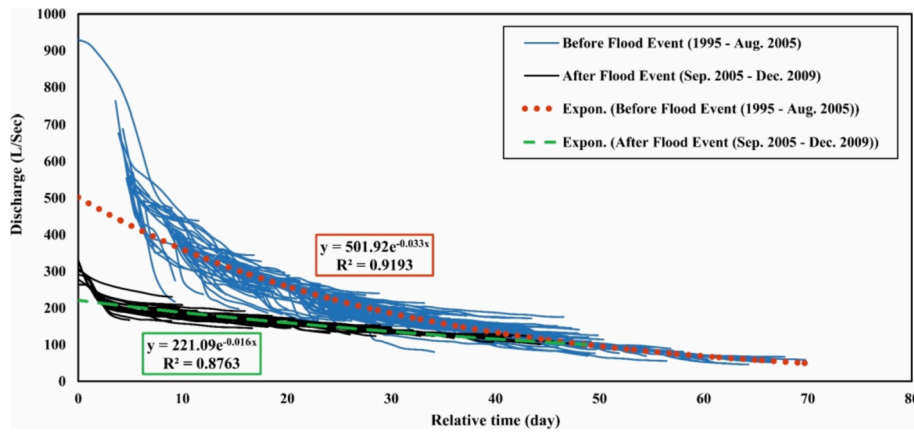


Fig. 7. Master recession curves of the Hammerbach spring during the period 1995 to 2009. Changed recession behavior within the period 2005–2009 (Mayaud et al., 2016) (Master recession curves were constructed with the method according to Posavec et al., 2006).

such that a considerable portion of this amount (85 %) is recharged during the observation period (Fig. 4-c). As shown by the modeling results, this results in a reduced recession coefficient during the observation period. Since recharge ceases during the extrapolation period the recession coefficient increases relative to that of the observation period. Therefore, the calculated remaining dynamic volume is higher than the actual volume. Daily discharge and weekly water table data from Galusquelle karst aquifer show that after reaching the maximum discharge the water table still rises (Fig. 8). This suggests ongoing recharge during the recession period and if this recharge ceases during late times, the recession coefficient will increase from that time onwards.

The spring discharge also decreases quicker during the extrapolation period than the exponential decline fitted to the observed recession period if specific yield or catchment area of the karst aquifer decrease with depth such as in scenarios S₁₃ and S₁₅ (Supplement 1). This is due to a decrease in storage when the groundwater level gradually decreases during the recession period. Thus, these conditions lead to an over-estimation of the remaining dynamic volume.

In scenario S₁₁, the hydraulic conductivity of the matrix gradually decreases towards the spring. This scenario shows that during the

extrapolation period spring discharge decreases more quickly than the exponential decline fitted to the observed recession period (Supplement 1). As the low-conductivity area close to the spring controls discharge during the observed recession period, groundwater initially drains slowly from the karst aquifer. However, after this part of aquifer has been drained, the high-conductivity area at the remote area of the aquifer controls the flow of groundwater. Fast groundwater drainage from this area causes the discharge during the extrapolation period to decrease faster than the curve extrapolated from the observed recession period. Thus, the remaining dynamic volume is overestimated.

Karst aquifers in Iran and many other regions of the world are used for the abstraction of drinking water by pumping wells. According to the S₇ scenario results, groundwater abstraction from the karst aquifer can also result in an acceleration of the discharge recession. The results of scenario S₇ show a strong decrease in spring discharge during the extrapolation period compared to the exponential decline fitted to the observed recession period. As a consequence, the estimated remaining dynamic volume will be larger than the actual value. This finding appears to be of high practical relevance for two reasons. First, the effects of groundwater abstraction may not only be caused by pumping within

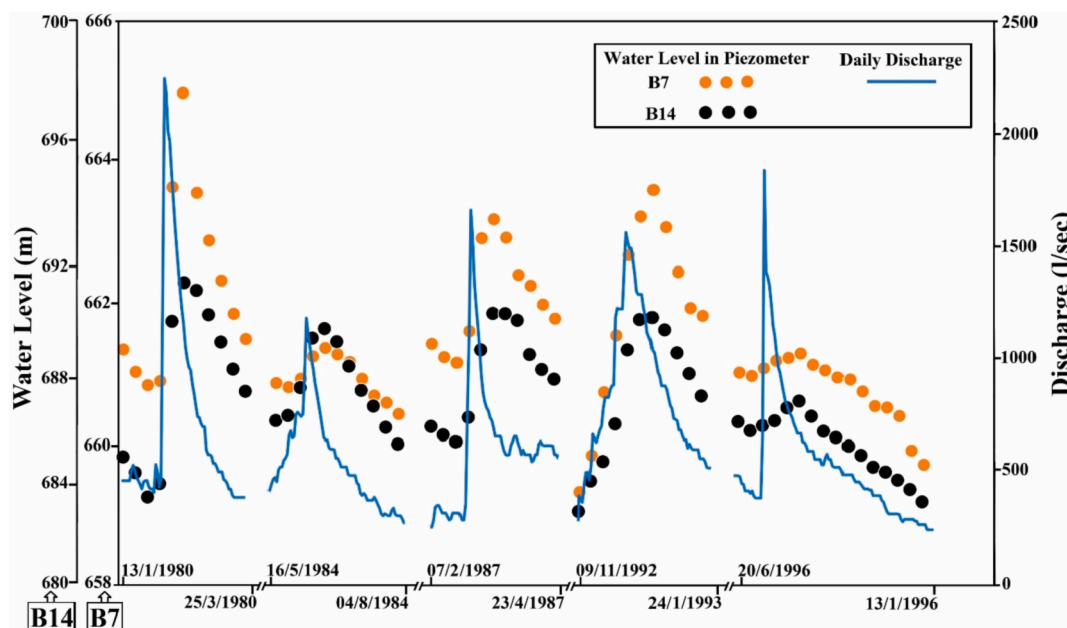


Fig. 8. Rising groundwater level in B7 and B14 piezometers after peak discharge of the Gallusquelle spring indicate ongoing recharge to the phreatic zone (Sauter, 1992).

the karst aquifer itself, but may result from the groundwater abstraction in adjacent karst or alluvial aquifers hydraulically connected but easily overlooked in the management of groundwater resources. Second, given the negligible effect on the recession coefficient observed for the early recession period, this may suggest that groundwater abstraction by pumping may not have relevant effects on spring discharge for average flow conditions, such that it is overlooked that the recession coefficient markedly increases during the extrapolation period. As a result, the groundwater resources will be unexpectedly vulnerable to drought conditions.

4.4. Overview of factors affecting the volume estimation

Table 4 presents a summary of the effects of the various factors on the dynamic volume estimation. This overview may serve as a checklist for a first assessment of potential underestimation or overestimation of the water storage estimated from the recession period. Whether or not the effects on the recession curve and thus on the volume estimate are significant will need more detailed field investigation and model application at the specific study site. In a real karst aquifer, some of the parameters examined here may simultaneously affect the estimation of the dynamic volume. If the individual parameters act in the same direction (overestimation or underestimation), their superposition is expected to increase the overall difference between the estimated and actual dynamic volume. In contrast, parameters that have opposing effects on the recession coefficient and thus the volume estimate may compensate each other partially or completely. The insight provided by model scenarios discussed here and summarized in Table 4 thus can guide investigations into such more complex settings.

5. Conclusion

Process-based modeling employing groundwater flow models was performed to simulate the hydrograph of typical karst springs. The behavior of the spring discharge pattern was analyzed during all stages of the recession period. Modelled aquifer parameters can easily be

Table 4
Influence of different parameters on dynamic volume estimation based on observed recession coefficient.

Parameter	Underestimation	Good Estimation	Overestimation
Point recharge		✓	
Geometry of the catchment area (L/W ratio)		✓	
High critical Reynolds number and hydraulic conductivity in the conduit	✓		
Highly conductive zone (conduit) only near the spring	✓		
Change in (increase and decrease) matrix hydraulic conductivity with depth of the aquifer	✓		
Increase in matrix hydraulic conductivity along the aquifer toward spring	✓		
Increase in catchment area or specific yield with depth of the aquifer	✓		
Ongoing recharge			✓
Decrease in catchment area or specific yield with depth of the aquifer			✓
Decrease of matrix hydraulic conductivity along the aquifer toward spring			✓
Groundwater abstraction			✓

changed to detect their effect on the different stages of the spring recession period. This was found helpful to investigate the effect of a change in each parameter on the different stages of the spring discharge recession.

The exact values of overestimation and underestimation dynamic volume of the modeled scenarios are summarized in the result section for comparison. These values can be expected to vary between different types of karst aquifers. Therefore, these numbers should not be taken as indicators of the relative importance of the different parameters. Instead, they illustrate the general effect of the individual parameters with respect to an over- or underestimation of the dynamic volume.

The results of this modelling study reveal that the dynamic volume estimation based on observed discharge recession, especially for aquifers that do not display long dry seasons, may not always yield reliable estimates, because the late times of the recession cannot be observed. In general, the best way to calculate the dynamic volume and extrapolate the recession coefficient is to build a master recession curve involving spring recessions for dry and very dry seasons. Should it be not possible to follow this suggested procedure, the results provided here can possibly support the assessment of the reliability of the estimate and may indicate a tendency towards overestimation or underestimation based on the knowledge of the hydrogeological characteristics of the catchment.

This study focused on unconfined aquifers that are drained by a spring at the aquifer base. While this type of setting is relevant in many water resources investigations, other types deserve attention too. For example, the development of conduit systems below the spring level may create deep and complex flow systems such as those feeding the Fontaine de Vaucluse spring in France (Fleury et al., 2007). Caution is needed when transferring our results to such different settings, and thus further investigations into the parameters controlling the dynamic volume and its estimation under conditions other than those considered here are recommended.

Finally, an important caveat, the discharge recession provides integral information on the entire aquifer system, i.e. the summed effects of spatio-temporal distribution of recharge, the hydraulic effects of the different compartments, i.e. epikarst, vadose zone and phreatic zone, as well as the effect of the partitioning of the flow between highly and less permeable systems. Thus, the variation of the individual aquifer geometries in horizontal and vertical directions, the variation of the above hydraulic parameters as well as other factors, their effect on system hydraulics are all summed up in just one individual recession curve, difficult to deconvolute. This implies a major ambiguity problem in the characterization of a karst system, which can be resolved only by using additional information, may it be soft (e.g. information on the genesis of the aquifer system) or hard (e.g. hydraulic conductivity of the matrix from pumping tests) data. Nevertheless, we suggest that the above systematic investigation helps approach the characterization of karst aquifers by recession analysis and assists in the analysis of less investigated karst systems where only information on spring discharge is available.

CRediT authorship contribution statement

Mahmoud Abirifard: Conceptualization, Methodology, Formal analysis, Writing – original draft. **Steffen Birk:** Conceptualization, Methodology, Writing – review & editing, Supervision. **Ezzat Raeisi:** Conceptualization, Writing – review & editing, Supervision. **Martin Sauter:** Conceptualization, Writing – review & editing, Supervision.

Declaration of Competing Interest

The authors declare that they have no known competing financial interests or personal relationships that could have appeared to influence the work reported in this paper.

Data availability

Data will be made available on request.

Acknowledgements

The first author would like to acknowledge Shiraz University for the continued support and thanks also go to the Ministry of Science, Research, and Technology, of Iran for supporting a six months' research of the first author at the Graz University. The authors acknowledge the financial support by the University of Graz.

Appendix A. Supplementary data

Supplementary data to this article can be found online at <https://doi.org/10.1016/j.jhydrol.2022.128286>.

References

- Atkinson, T.C., 1977. Diffuse flow and conduit flow in limestone terrain in the Mendip Hills, Somerset (Great Britain). *J. Hydrol.* 35, 93–110. [https://doi.org/10.1016/0022-1694\(77\)90079-8](https://doi.org/10.1016/0022-1694(77)90079-8).
- Baedke, S.J., Krothe, N.C., 2001. Derivation of effective hydraulic parameters of a karst aquifer from discharge hydrograph analysis. *Water Resour. Res.* 37, 13–19. <https://doi.org/10.1029/2000WR900247>.
- Bakalowicz, M., 2005. Karst groundwater: A challenge for new resources. *Hydrogeol. J.* 13, 148–160. <https://doi.org/10.1007/s10040-004-0402-9>.
- Barmaki, M.D., Rezaei, M., Raeisi, E., Ashjari, J., 2019. Comparison of surface and interior karst development in Zagros Karst Aquifers. *Southwest Iran. J. Cave Karst Stud.* 81, 84–97. <https://doi.org/10.4311/2017es0120>.
- Birk, S., Hergarten, S., 2010. Early recession behaviour of spring hydrographs. *J. Hydrol.* 387, 24–32. <https://doi.org/10.1016/j.jhydrol.2010.03.026>.
- Birk, S., Liedl, R., Sauter, M., 2006. Karst spring responses examined by process-based modeling. *Ground Water* 44, 832–836. <https://doi.org/10.1111/j.1745-6584.2006.00175.x>.
- Bonacci, O., 1993. Karst springs hydrographs as indicators of karst aquifers. *Hydrol. Sci. J.* 38, 51–62. <https://doi.org/10.1080/02626669309492639>.
- Dewandel, B., Lachassagne, P., Bakalowicz, M., Weng, P., Al-Malki, A., 2003. Evaluation of aquifer thickness by analysing recession hydrographs. Application to the Oman ophiolite hard-rock aquifer. *J. Hydrol.* 274, 248–269. [https://doi.org/10.1016/S0022-1694\(02\)00418-3](https://doi.org/10.1016/S0022-1694(02)00418-3).
- Einsiedl, F., 2005. Flow system dynamics and water storage of a fissured-porous karst aquifer characterized by artificial and environmental tracers. *J. Hydrol.* 312, 312–321. <https://doi.org/10.1016/j.jhydrol.2005.03.031>.
- Eisenlohr, L., Király, L., Bouzelboudjen, M., Rossier, Y., 1997. Numerical simulation as a tool for checking the interpretation of karst spring hydrographs. *J. Hydrol.* 193, 306–315. [https://doi.org/10.1016/S0022-1694\(96\)03140-X](https://doi.org/10.1016/S0022-1694(96)03140-X).
- El-Hakim, M., Bakalowicz, M., 2007. Significance and origin of very large regulating power of some karst aquifers in the Middle East. Implication on karst aquifer classification. *J. Hydrol.* 333, 329–339. <https://doi.org/10.1016/j.jhydrol.2006.09.003>.
- Fiorillo, F., 2014. The Recession of Spring Hydrographs. Focused on Karst Aquifers. *Water Resour. Manag.* 28, 1781–1805. <https://doi.org/10.1007/s11269-014-0597-z>.
- Fiorillo, F., 2011. Tank-reservoir drainage as a simulation of the recession limb of karst spring hydrographs. *Hydrogeol. J.* 19 (5), 1009–1019.
- Fiorillo, F., Revellino, P., Ventafredda, G., 2012. Karst aquifer draining during dry periods. *J. Cave Karst Stud.* 74, 148–156. <https://doi.org/10.4311/2011JCKS0207>.
- Fleury, P., Plagnes, V., Bakalowicz, M., 2007. Modelling of the functioning of karst aquifers with a reservoir model: Application to Fontaine de Vaulcuse (South of France). *J. Hydrol.* 345, 38–49. <https://doi.org/10.1016/j.jhydrol.2007.07.014>.
- Ford, D., Williams, P., 2007. Karst hydrogeology and geomorphology.
- Forkasiewicz, J., Paloc, H., 1967. Le régime de tarissement de la Foux de la Vis étude préliminaire. In: *Proceedings of the Dubrovnik Symposium*, October 1965. Hydrology of Fractured Rocks, 1, 213–226.
- Fu, T., Chen, H., Wang, K., 2016. Structure and water storage capacity of a small karst aquifer based on stream discharge in southwest China. *J. Hydrol.* 534, 50–62. <https://doi.org/10.1016/j.jhydrol.2015.12.042>.
- Hartmann, A., Lange, J., Vivó Aguado, A., Mizyed, N., Smiatek, G., Kunstmann, H., 2012. A multi-model approach for improved simulations of future water availability at a large Eastern Mediterranean karst spring. *J. Hydrol.* 468–469, 130–138. <https://doi.org/10.1016/j.jhydrol.2012.08.024>.
- Jukić, D., Denić-Jukić, V., 2009. Groundwater balance estimation in karst by using a conceptual rainfall-runoff model. *J. Hydrol.* 373, 302–315. <https://doi.org/10.1016/j.jhydrol.2009.04.035>.
- Karimi, H., Raeisi, E., Zare, M., 2003. Hydrodynamic behavior of the Gilan karst spring, west of the Zagros. *Iran. Cave Karst Sci.* 30, 15–22.
- Kavousi, A., Raeisi, E., 2015. Estimation of groundwater mean residence time in unconfined karst aquifers using recession curves. *J. Cave Karst Stud.* 77, 108–119. <https://doi.org/10.4311/2014ES0106>.
- Kogovsek, J., 1997. Water tracing tests in the vadose zone. In: *Kranjc, A. (Ed.), Tracer Hydrology* 97. Balkema, Rotterdam, pp. 167–172.
- Kovács, A., Perrochet, P., Király, L., Jeannin, P.Y., 2005. A quantitative method for the characterisation of karst aquifers based on spring hydrograph analysis. *J. Hydrol.* 303, 152–164. <https://doi.org/10.1016/j.jhydrol.2004.08.023>.
- Kuniansky, E.L., Halford, K.J., Shoemaker, W.B., 2008. Permeameter data verify new turbulence process for MODFLOW. *Ground Water* 46, 768–771. <https://doi.org/10.1111/j.1745-6584.2008.00458.x>.
- Lastennet, R., Mudry, J., 1997. Role of karstification and rainfall in the behavior of a heterogeneous karst system. *Environ. Geol.* 32, 114–123. <https://doi.org/10.1007/s002540050200>.
- Maillet, E.T., 1905. *Essais d'hydraulique souterraine et fluviale*. A. Hermann.
- Maloszewski, P., Stichler, W., Zuber, A., Rank, D., 2002. Identifying the flow systems in a karstic-fissured-porous aquifer, the schneepalpe, Austria, by modelling of environmental ^{18}O and ^3H isotopes. *J. Hydrol.* 256, 48–59. [https://doi.org/10.1016/S0022-1694\(01\)00526-1](https://doi.org/10.1016/S0022-1694(01)00526-1).
- Mangin, A., 1975. *Contribution à l'étude hydrodynamique des aquifères karstiques*. Laboratoire souterrain du Centre national de la recherche scientifique.
- Mayaud, C., Wagner, T., Benischke, R., Birk, S., 2016. Understanding changes in the hydrological behaviour within a karst aquifer (Lurbach system, Austria). *Carbonates Evaporites* 31, 357–365. <https://doi.org/10.1007/s13146-013-0172-3>.
- Mohammadi, Z., Shoja, A., 2014. Effect of annual rainfall amount on characteristics of karst spring hydrograph. *Carbonates Evaporites* 29, 279–289. <https://doi.org/10.1007/s13146-013-0175-0>.
- Naderi, M., Raeisi, E., 2015. Climate change in a region with altitude differences and with precipitation from various sources, South-Central Iran. *Theor. Appl. Climatol.* 124, 529–540. <https://doi.org/10.1007/s00704-015-1433-y>.
- Olariño, T., Gleeson, T., Marx, V., Seeger, S., Adinehvand, R., Allocca, V., Andreo, B., Apaestegui, J., Apoliti, C., Arfib, B., Auler, A., Bailly-Comte, V., Barberá, J.A., Batiot-Guilhe, C., Bechtel, T., Binet, S., Bittner, D., Blatnik, M., Bolger, T., Brunet, P., Charlier, J.-B., Chen, Z., Chiogna, G., Coxon, G., De Vita, P., Doummar, J., Epting, J., Fleury, P., Fournier, M., Goldscheider, N., Gunn, J., Guo, F., Guyot, J.L., Howden, N., Huggenberger, P., Hunt, B., Jeannin, P.-Y., Jiang, G., Jones, G., Jourde, H., Karmann, I., Koit, O., Kordilla, J., Labat, D., Ladouche, B., Liso, I.S., Liu, Z., Maréchal, J.-C., Massei, N., Mazzilli, N., Mudarra, M., Parise, M., Pu, J., Ravbar, N., Sanchez, L.H., Santo, A., Sauter, M., Seidel, J.-L., Sivel, V., Skoglund, R.Ö., Stevanovic, Z., Wood, C., Worthington, S., Hartmann, A., 2020. Global karst springs hydrograph dataset for research and management of the world's fastest-flowing groundwater. *Sci. Data* 7 (1). <https://doi.org/10.1038/s41597-019-0346-5>.
- Padilla, A., Pulido-Bosch, A., Mangin, A., 1994. Relative importance of Baseflow and Quickflow from Hydrographs of Karst Spring. *Groundwater* 32 (2), 267–277.
- Pérez, J.J., Sanz, E., 2011. Hydrodynamic characteristics and sustainable use of a karst aquifer of high environmental value in the Cabrejas range (Soria, Spain). *Environ. Earth Sci.* 62, 467–479. <https://doi.org/10.1007/s12665-010-0540-4>.
- Perrin, J., 2003. *A conceptual model of flow and transport in a karst aquifer based on spatial and temporal variations of natural tracers*. Université de Neuchâtel. Doctoral dissertation.
- Posavec, K., Bačani, A., Nakić, Z., 2006. A visual basic spreadsheet macro for recession curve analysis. *Ground Water* 44, 764–767. <https://doi.org/10.1111/j.1745-6584.2006.00226.x>.
- Raeisi, E., Karami, G., 1997. Hydrochemographs of Berghan karst spring as indicators of aquifer characteristics. *J. Cave Karst Stud.* 59, 112–118.
- Raeisi, E., Pezeshkpoor, P., Moor, F., 1993. Characteristics of karst aquifer as indicated by temporal changes of the spring's physico-chemical parameters. *Iran. J. Sci. Technol.* 17, 17–28.
- Reimann, T., Rehr, C., Shoemaker, W.B., Geyer, T., Birk, S., 2011. The significance of turbulent flow representation in single-continuum models. *Water Resour. Res.* 47, 1–15. <https://doi.org/10.1029/2010WR010133>.
- Sauter, M., 1992. Quantification and forecasting of regional groundwater flow and transport in a karst aquifer (Gallusquelle, Malm, SW. Germany). *Tübinger Geowissenschaftliche Arbeiten, Reihe C*, 13, Tübingen.
- Sauter, M., 1995. Delineation of a karst aquifer using geological and hydrological data and information on landscape development. *Carbonates Evaporites* 10, 129–139. <https://doi.org/10.1007/BF03175401>.
- Shoemaker, W.B., Kuniansky, E.L., Birk, S., Bauer, S., Swain, E.D., 2008. *Documentation of a Conduit Flow Process (CFP) for MODFLOW-2005*. U.S. Geol. Surv. Tech. Methods, B. 6 chapter A24 50.
- Smart, P.L., Friederich, H., 1987. In: *Water movement and storage in the unsaturated zone of a maturely karstified carbonate aquifer, Mendip Hills, England*. National Water Well Association, Dublin, Ohio, pp. 59–87.
- Smart, P.L., Hobbs, S.L., 1986. Characterization of carbonate aquifers; a conceptual base. In *Proceedings of the Environmental Problems in Karst Terranes and Their Solutions Conference*, Bowling Green, Kentucky, National Water Well Association, Dublin, Ohio, 1–14.
- Wu, P., Shu, L., Li, F., Chen, H., Xu, Y., Zou, Z., Mabedi, E.C., 2019. Impacts of artificial regulation on karst spring hydrograph in Northern China: Laboratory study and numerical simulations. *Water (Switzerland)* 11, 755. <https://doi.org/10.3390/w11040755>.
- Željковиć, I., Kadić, A., 2015. Groundwater balance estimation in karst by using simple conceptual rainfall-runoff model. *Environ. Earth Sci.* 74, 6001–6015. <https://doi.org/10.1007/s12665-015-4624-z>.